*Journal of Sound and Vibration* (2001) **243**(4), 679–697
doi:10.1006/jsvi.2000.3445, available online at http://www.idealibrary.com on IDEAL®

# SPECIFIC FEATURES OF THE ACOUSTIC DIFFRACTION FROM A PERIODIC SYSTEM OF PLANAR SLIDING-CONTACT INTERFACES

A. L. Shuvalov and A. S. Gorkunova

*Institute of Crystallography, Russian Academy of Sciences, Leninskii pr.* 59, *Moscow* 117333, *Russia.*
*E-mail: ashuv@ns.crys.ras.ru*

(*Received* 7 *February* 2000, *and in final form* 4 *September* 2000)

Propagation of sagittally polarized plane acoustic waves is considered in an orthorhombic medium with a periodic system of $N+1$ infinite planar cuts maintaining sliding contact (ideal cracks). The reflection and transmission rates are derived by the propagator-matrix method. Two essentially different types of stop bands exist, in which the imaginary part of the Bloch vector either remains finite or reaches infinity. The latter corresponds to the transmission cut-off, which may come about specifically at the sliding-contact interface. Coupling of the Bragg phenomenon with the cutting-off effect produces quite specific resonant features of reflection and transmission. Especially sharp filtering properties of the spectra come about at a small deviation $\Delta\theta$ from such angles of incidence, which provide total transmission (anti-reflection) independent of frequency, namely, at nearly normal incidence of the fast mode, and at angles of incidence of the slow mode close to a certain critical value. At $|\Delta\theta| \ll 1$, the spectrum of transmission (without mode conversion) represents a nearly periodic group of abrupt dips to zero and a modulated group of secondary drops increasing with growing $(\Delta\theta)^2 N^2$, whereas the general spectral background is close to unity. In turn, the reflection spectrum at $|\Delta\theta| \ll 1$ contains sharp principal peaks with modulated heights, reaching nearly unit height, and the secondary peaks against almost zero background. Changes in the spectra shape on varying the angle of incidence $\theta$ become drastic near the specific threshold value of $\theta$, which corresponds to the mutual transformation of the ordinary stop bands and cutting-off bands. After the cross-over, the transmission spectrum contains significantly wide step-wise dips, within which the rate stays very close to zero if $N^2 \gg 1$.



## 1. INTRODUCTION

The physical type of contact provided along a planar interface between two solids is known to be one of the key factors in determining acoustic response from this interface. Various linear models of interfacial contact can be interpreted in terms of the relation between the relative tangential displacement (slip) along the interface and the shear stresses, so that a perfect bonding corresponds to the absence of slip, while the opposite extreme is the case of a sliding contact, incapable of supporting shear stresses. The sliding type of contact models a perfectly lubricated interface, or a narrow crack filled with an inviscid fluid layer. It may also be viewed as a common long-wavelength limit for different types of mixed boundary conditions between "loosely bonded" solids, for which the factor between the interfacial slip and the shear stresses is inversely proportional to the frequency (see, e.g. reference [1]).

Acoustic properties of a sliding-contact interface have been studied by many authors with respect to non-destructive material characterization and seismic-wave propagation.

0022-460X/01/240679 + 19 $35.00/0 

A significant distinction in the case of perfect bonding has been revealed in the properties of localized interface waves [2], and in the nature of reflection–transmission [3]. Regarding the latter problem, it was shown that a specific attribute of a sliding-contact interface is the possibility of vanishing transmission of a plane acoustic wave (cutting-off effect), so that neither bulk, nor inhomogeneous modes are transmitted through such an interface into any adjoining half-space for particular angles of incidence (which may be less than the angle of total reflection), or for particular frequencies if there is an intermediate layer in sliding contact with two arbitrary substrates. At the same time, it was also found that the sliding-contact interface between identical half-spaces brings about total transmission (antireflection) for certain angles of incidence.

The present paper studies the diffraction of sagittally polarized acoustic waves in an orthorhombic medium with an embedded periodic system of sliding-contact interfaces. Such a medium can be arranged by gluing together identical layers with the aid of a low-viscosity lubricant occupying a sufficiently thin (compared to the wavelength) space between the layers. Although much work has been done for composite structures with rigid contact at interfaces (see reference [4]), little work appear to deal with systems of layers in sliding contact. However, the aforementioned remarkable nature of the reflection–transmission at a single sliding-contact interface and a single sliding intermediate layer suggests the possibility of striking features of the diffraction in a periodic structure with sliding-contact interfaces. Indeed, a drastic transformation of the diffraction spectrum should be expected with a small deviation of the angle of incidence from the angle of total transmission, when the transmission cut-off and the Bragg effect instantly come into play, providing an abrupt increase of reflection at certain frequencies. In a broader perspective, it seems fundamentally interesting to explore the coupling between the cutting-off effect, stipulated by the sliding contact, and the Bragg-resonance phenomenon. As will be shown, this endows novel aspects to the concept of Bloch stop bands and the ensuing properties of the diffraction.

## 2. BACKGROUND

Consider a stack of $N$ identical orthorhombic elastic layers of width $h$ in sliding contact along interfaces, which is bounded on both sides by semi-infinite substrates made from the same material as the layers. The structure may be also viewed as a single medium with an equidistant system of thin planar cuts or cracks (their width being much less than the wavelength), which are filled with an inviscid fluid. Both the interfaces and the plane orthogonal to them (the sagittal plane) are assumed to coincide with symmetry planes. The co-ordinate axes are chosen so that the interface plane is $ZX$, the sagittal plane is $XY$, and the axis $Y$ is orthogonal to the interfaces (Figure 1). The sagittally polarized displacement field in the $n$th layer may be written in the form

$$\mathbf{u}^{(n)} = \sum_{\alpha=1}^{4} b_\alpha^{(n)} \mathbf{a}_\alpha e^{i\varphi_\alpha}, \quad \varphi_\alpha = k_x x + k_{\alpha y}(y + nh) - \omega t, \tag{1}$$

where $b_\alpha^{(n)}$ are partial scalar amplitudes; $\mathbf{a}_\alpha$ are the polarization vectors orthogonal to $Z$. The equation of motion yields the dispersion relation for the sagittal modes $\alpha = 1, \ldots, 4$, referred to a given $k_x$. Provided that $k_x \neq 0$, it may be written in terms of parameters

$$p_\alpha = \frac{k_{\alpha y}}{k_x}, \quad v = \frac{\omega}{k_x} \tag{2}$$

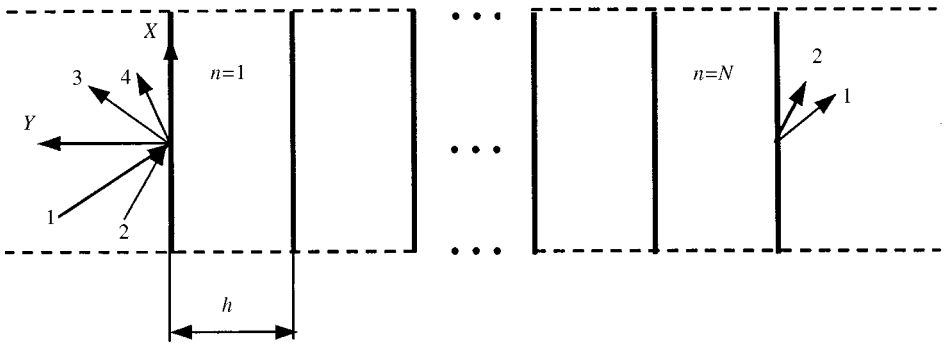


Figure 1. Geometry of the problem. Numbers label partial modes $\alpha = 1, 2, 3, 4$.

in the form (see, e.g., references [4, 5])

$$p_\alpha^2 = \frac{1}{2c_{22}c_{66}}\{\rho v^2(c_{22}+c_{66}) - c_{11}c_{22} + c_{12}^2 + 2c_{12}c_{66} \pm \sqrt{[\rho v^2(c_{22}+c_{66}) - c_{11}c_{22} + c_{12}^2 + 2c_{12}c_{66}]^2 - 4c_{22}c_{66}(\rho v^2 - c_{11})(\rho v^2 - c_{66})}\}, \tag{3}$$

where $\rho$ is the density and $c_{ab}$ are elastic coefficients in Voigt's notations. Let the subscripts $\alpha = 1, 3$ and $2, 4$ be associated, respectively, with the signs "+" (the slow wave branch) and "−" (the fast wave branch). Given that $c_{11} > c_{66}$, the modes $\alpha = 2, 4$ are inhomogeneous ($p_{2,4}^2 < 0$) at $v^{-1} > \sqrt{\rho/c_{11}}$, and so are the modes $\alpha = 1, 3$ at $v^{-1} > \sqrt{\rho/c_{66}}$, unless the section of the outer slowness sheet, related to the slow sagittal wave branch, is concave around the $X$-axis. In the latter case, conditioned by the inequality $(c_{12}+c_{66})^2 > c_{22}(c_{11}-c_{66})$ [6, 7], the sagittal modes $\alpha = 1, \ldots, 4$ are homogeneous (bulk) in the range $\sqrt{\rho/c_{66}} < v^{-1} < v_L^{-1}$, where $v_L$ nullifies the radical in equation (3). Once the modes are homogeneous, the subscripts $\alpha = 1, 2$ are assigned to the incident modes and $n = 3, 4$ to the reflected ones (i.e., the modes with, respectively, negative and positive $y$-components of the energy fluxes $P_{\alpha y}$). The relation between the variable $v$ and the angle of incidence of the mode $\alpha = 1$ or 2 is furnished by the relation $\theta_\alpha = \operatorname{arccot}[p_\alpha(v)]$.

The (unnormalized) polarization vectors $\mathbf{a}_\alpha$ and the amplitudes $\mathbf{l}_\alpha$ of corresponding surface tractions $\sigma_{2j}^{(\alpha)} = -\mathrm{i}k_x l_{\alpha i}\mathrm{e}^{\mathrm{i}\varphi_\alpha}$ ($k_x \neq 0$), exerted by partial displacements, may be written in the form [4, 5]

$$\mathbf{a}_1 = \begin{pmatrix} a_{1x} \\ a_{1y} \end{pmatrix}, \quad \mathbf{a}_2 = \begin{pmatrix} a_{2x} \\ a_{2y} \end{pmatrix}, \quad \mathbf{a}_3 = \begin{pmatrix} -a_{1x} \\ a_{1y} \end{pmatrix}, \quad \mathbf{a}_4 = \begin{pmatrix} -a_{2x} \\ a_{2y} \end{pmatrix},$$

$$\mathbf{l}_1 = \begin{pmatrix} l_{1x} \\ l_{1y} \end{pmatrix}, \quad \mathbf{l}_2 = \begin{pmatrix} l_{2x} \\ l_{2y} \end{pmatrix}, \quad \mathbf{l}_3 = \begin{pmatrix} l_{1x} \\ -l_{1y} \end{pmatrix}, \quad \mathbf{l}_4 = \begin{pmatrix} l_{2x} \\ -l_{2y} \end{pmatrix}, \tag{4}$$

where

$$a_{\alpha x} = -(c_{12}+c_{66})p_\alpha, \quad a_{\alpha y} = \rho v^2 - c_{11} - c_{66}p_\alpha^2,$$

$$l_{\alpha x} = -c_{66}(\rho v^2 - c_{11} + c_{12}p_\alpha^2), \qquad \alpha = 1, 2, \tag{5}$$

$$l_{\alpha y} = p_\alpha[c_{12}(c_{12}+c_{66}) + c_{22}(\rho v^2 - c_{11} - c_{66}p_\alpha^2)],$$

In the case of normal propagation ($k_x = 0$), the four-partial wave packet consists of longitudinal and transverse modes, which exert tractions parallel to the polarizations.

The Stroh-normalized polarizations $\mathbf{A}_\alpha = C_\alpha \mathbf{a}_\alpha$ and traction amplitudes $\mathbf{L}_\alpha = C_\alpha \mathbf{l}_\alpha$ may be introduced according to the definition $2\mathbf{A}_\alpha \cdot \mathbf{L}_\alpha = 1$ ($\alpha = 1, \ldots, 4$) [5]. It follows that

$$C_\alpha^2 = \frac{1}{2(\mathbf{a}_\alpha \cdot \mathbf{l}_\alpha)}, \quad C_{\alpha+2} = \mathrm{i} C_\alpha, \quad \alpha = 1, 2, \tag{6}$$

where $C_\alpha$ are real for bulk modes $\alpha = 1, 2$, characterized by the negative normal component of the energy flux $P_{\alpha y} = -(\omega k_x/2)\mathbf{a}_\alpha \cdot \mathbf{l}_\alpha$.

## 3. CALCULATION OF THE REFLECTION AND TRANSMISSION COEFFICIENTS

The boundary conditions at the sliding-contact interface prescribe vanishing of tangential traction and continuity of normal displacement and traction. The former requirement may be written at both interfaces of the $n$th layer in the form

$$\begin{aligned} &b_1^{(n)} l_{1x} \mathrm{e}^{-\mathrm{i}k_{1y}h} + b_2^{(n)} l_{2x} \mathrm{e}^{-\mathrm{i}k_{2y}h} + b_3^{(n)} l_{1x} \mathrm{e}^{\mathrm{i}k_{1y}h} + b_4^{(n)} l_{2x} \mathrm{e}^{\mathrm{i}k_{2y}h} = 0, \\ &b_1^{(n)} l_{1x} + b_2^{(n)} l_{2x} + b_3^{(n)} l_{1x} + b_4^{(n)} l_{2x} = 0. \end{aligned} \tag{7}$$

The condition of continuity of normal components across the interface between the $n$th and $(n+1)$th layers implies that

$$\begin{aligned} &b_1^{(n)} a_{1y} + b_2^{(n)} a_{2y} + b_3^{(n)} a_{1y} + b_4^{(n)} a_{2y} \\ &\quad = b_1^{(n+1)} a_{1y} \mathrm{e}^{-\mathrm{i}k_{1y}h} + b_2^{(n+1)} a_{2y} \mathrm{e}^{-\mathrm{i}k_{2y}h} + b_3^{(n+1)} a_{1y} \mathrm{e}^{\mathrm{i}k_{1y}h} + b_4^{(n+1)} a_{2y} \mathrm{e}^{\mathrm{i}k_{2y}h}, \\ &b_1^{(n)} l_{1y} + b_2^{(n)} l_{2y} - b_3^{(n)} l_{1y} - b_4^{(n)} l_{2y} \\ &\quad = b_1^{(n+1)} l_{1y} \mathrm{e}^{-\mathrm{i}k_{1y}h} + b_2^{(n+1)} l_{2y} \mathrm{e}^{-\mathrm{i}k_{2y}h} - b_3^{(n+1)} l_{1y} \mathrm{e}^{\mathrm{i}k_{1y}h} - b_4^{(n+1)} l_{2y} \mathrm{e}^{\mathrm{i}k_{2y}h}. \end{aligned} \tag{8}$$

It is seen that the method of a propagator matrix in the form devised for the rigid-contact multilayers, when displacements and tractions are continuous across the interfaces (e.g., references [4, 8], see also reference [9] for the case of weak bonding), cannot be straightforwardly applied to the sliding-contact multilayers. Indeed, the condition of zero tangential tractions (equation (7)) precludes taking the inverse matrix needed for construction a $(4 \times 4)$ propagator matrix, such as would transfer the column of four partial amplitudes through the sliding-contact interface. However, this condition may be utilized to eliminate some of the partial modes from the remaining boundary conditions, which then yield the $2 \times 2$ propagator matrix. Such a modified matrix method was first worked out in reference [10] for the wave propagation in alternating solid and fluid layers. The same idea underlaid the consideration of the acoustic diffraction in piezoelectric or piezomagnetic superlattices with screening (metallized or superconducting) interfaces, at which electropotential or normal component of magnetic induction turns to zero [11].

Using equation (7), let the partial amplitudes of, say, the slow modes $\alpha = 1, 3$ be expressed in terms of the amplitudes of the fast ones $\alpha = 2, 4$ (such a choice fits the case of the mode

$\alpha = 2$ incidence), so that

$$\begin{pmatrix} b_1 \\ b_3 \end{pmatrix}^{(n)} = \frac{\mathrm{i}l_{2x}}{2l_{1x}\sin(k_{1y}h)} \begin{pmatrix} \mathrm{e}^{\mathrm{i}k_{1y}h} - \mathrm{e}^{-\mathrm{i}k_{2y}h} & \mathrm{e}^{\mathrm{i}k_{1y}h} - \mathrm{e}^{\mathrm{i}k_{2y}h} \\ \mathrm{e}^{-\mathrm{i}k_{2y}h} - \mathrm{e}^{-\mathrm{i}k_{1y}h} & \mathrm{e}^{\mathrm{i}k_{2y}h} - \mathrm{e}^{-\mathrm{i}k_{1y}h} \end{pmatrix} \begin{pmatrix} b_2 \\ b_4 \end{pmatrix}^{(n)}, \tag{9}$$

where the layer's number $n$ is arbitrary. Inserting equation (9) into both sides of equations (8) allows one to eliminate the amplitudes of the modes $\alpha = 1, 3$. As a result, the relation

$$\begin{pmatrix} b_2 \\ b_4 \end{pmatrix}^{(n)} = \mathbf{W} \begin{pmatrix} b_2 \\ b_4 \end{pmatrix}^{(n+1)} \tag{10}$$

is reached, where $\mathbf{W}$ is the $(2 \times 2)$ propagator matrix, transferring partial amplitudes of the modes $\alpha = 2, 4$ from one layer to another. It has the form

$$\mathbf{W} = \frac{1}{\chi + \chi^*} \begin{pmatrix} 2\chi \mathrm{e}^{-\mathrm{i}k_{2y}h} & (\chi - \chi^*)\mathrm{e}^{\mathrm{i}k_{2y}h} \\ (\chi^* - \chi)\mathrm{e}^{-\mathrm{i}k_{2y}h} & 2\chi^* \mathrm{e}^{\mathrm{i}k_{2y}h} \end{pmatrix}, \tag{11}$$

in which the notations

$$\chi = 1 - \mathrm{i}\eta \frac{(\mathrm{e}^{\mathrm{i}k_{2y}h} - \cos(k_{1y}h))}{\sin(k_{1y}h)} \tag{12}$$

are used and

$$\eta = -\frac{l_{1y}l_{2x}}{l_{1x}l_{2y}} = -\frac{L_{1y}L_{2x}}{L_{1x}L_{2y}} = \frac{L_{1y}^2}{L_{2y}^2} = \frac{L_{2x}^2}{L_{1x}^2}. \tag{13}$$

Typical patterns of the function $\eta(v^{-1})$, studied in reference [3], are presented in Figure 2, where

$$v_0^{-1} = \sqrt{\frac{\rho(c_{12} + c_{22})}{c_{11}c_{22} - c_{12}^2}} \tag{14}$$

and the dashed curve indicates purely imaginary values taken by $\eta$ in the interval $\sqrt{\rho/c_{11}} < v^{-1} < \sqrt{\rho/c_{66}}$. Note that the maximum of $\eta$ occurring at $v^{-1} < \sqrt{\rho/c_{11}}$ generally may or may not exceed unity (the case shown in Figure 2 is optional), which will appear significant in the subsequent analysis revealing the value $\eta = 1$ as a certain threshold of the angular dependence of the reflection–transmission spectra.

In accordance with the symmetry of the problem (see references [4, 12]), the matrix $\mathbf{W}$ is unimodular, i.e., $\det \mathbf{W} = 1$. Therefore, $\mathbf{W}$ possesses the eigenvalues $\mathrm{e}^{\mathrm{i}K_2h}$, $\mathrm{e}^{-\mathrm{i}K_2h}$, where $K_2$ is the Bloch wave number. It satisfies the dispersion relation

$$\cos(K_2h) = \cos(k_{2y}h) + \frac{(\cos(k_1h) - \cos(k_{2y}h))}{(\sin(k_{1y}h) + \eta\sin(k_{2y}h))} \eta \sin(k_{2y}h). \tag{15}$$

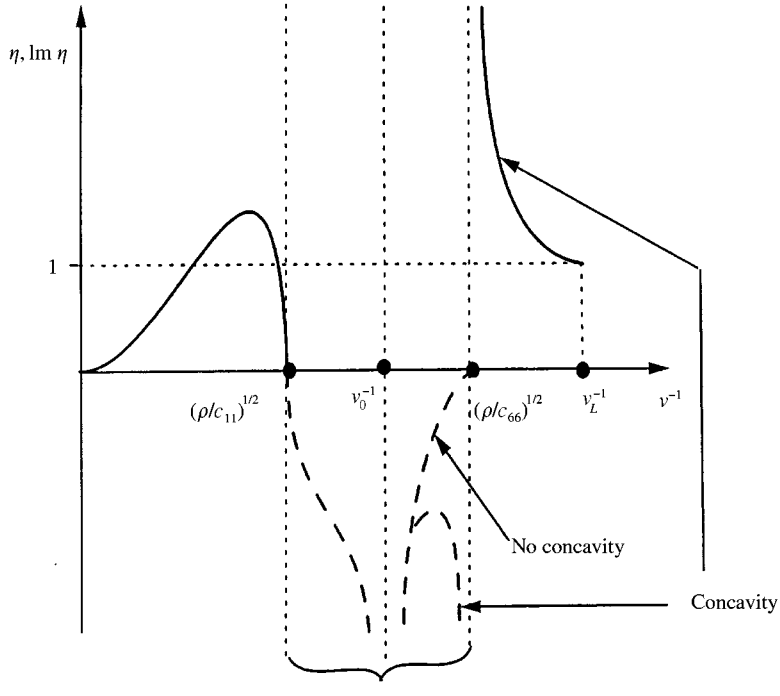
η, lm η
1
$(\rho/c_{11})^{1/2}$
$v_0^{-1}$
$(\rho/c_{66})^{1/2}$
$v_L^{-1}$
$v^{-1}$
No concavity
Concavity
lm η

(a)

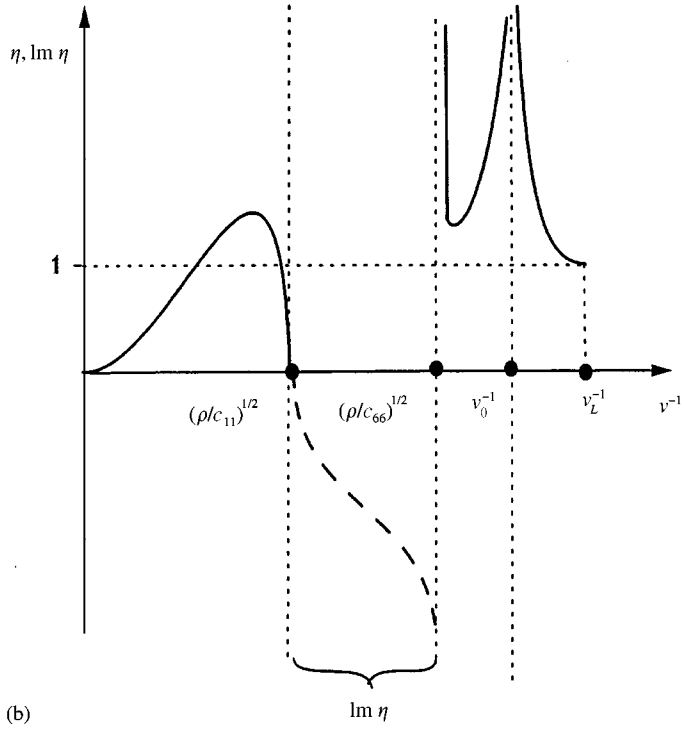
η, lm η
1
$(\rho/c_{11})^{1/2}$
$(\rho/c_{66})^{1/2}$
$v_0^{-1}$
$v_L^{-1}$
$v^{-1}$
lm η

(b)

The "entrance" and "exit" matrices $\mathbf{W}_{en}$ and $\mathbf{W}_{ex}$, transferring the amplitudes through substrate I—first layer interface and through the last ($N$th) layer—substrate II interface, differ from $\mathbf{W}$. Bearing in mind the choice of the fast mode ($\alpha = 2$) as the incident one, and implementing a similar elimination procedure as above, it is found that

$$\mathbf{W}_{en} = \frac{1}{2}\begin{pmatrix} (1+\eta+\chi)\mathrm{e}^{-\mathrm{i}k_{2y}h} & (1+\eta-\chi^*)\mathrm{e}^{\mathrm{i}k_{2y}h} \\ (1-\eta-\chi)\mathrm{e}^{-\mathrm{i}k_{2y}h} & (1-\eta+\chi^*)\mathrm{e}^{\mathrm{i}k_{2y}h} \end{pmatrix}, \tag{16}$$

$$\mathbf{W}_{ex} = \frac{1}{\chi+\chi^*}\begin{pmatrix} 1+\eta+\chi & -1+\eta+\chi \\ -1-\eta+\chi^* & 1-\eta+\chi^* \end{pmatrix}. \tag{17}$$

The amplitudes $b_2^{(\mathrm{I})}, b_4^{(\mathrm{I})}$ of the incident and reflected fast modes in substrate I are related to the amplitude $b_2^{(\mathrm{II})}$ of the fast mode transmitted through the multilayered structure into substrate II (Figure 1) by the relation

$$\begin{pmatrix} b_2 \\ b_4 \end{pmatrix}^{(\mathrm{I})} = \mathbf{W}_{en}\mathbf{W}^{N-1}\mathbf{W}_{ex}\begin{pmatrix} b_2 \\ 0 \end{pmatrix}^{(\mathrm{II})}, \tag{18}$$

where the $(N-1)$th power of the $2\times 2$ unimodular matrix $\mathbf{W}$ is given by the expression (see reference [13])

$$\mathbf{W}^{N-1} = \begin{pmatrix} W_{11}S_N^{(2)} - S_N^{(2)} & W_{12}S_N^{(2)} \\ W_{21}S_N^{(2)} & W_{22}S_N^{(2)} - S_N^{(2)} \end{pmatrix}, \tag{19}$$

in which

$$S_n^{(2)} = \frac{\sin(nK_2h)}{\sin(K_2h)}. \tag{20}$$

The partial coefficients of reflection and transmission are introduced in the form

$$r_3^{(2)} = \frac{b_3^{(\mathrm{I})}}{b_2^{(\mathrm{I})}}, \quad r_4^{(2)} = \frac{b_4^{(\mathrm{I})}}{b_2^{(\mathrm{I})}}, \quad t_1^{(2)} = \frac{b_1^{(\mathrm{II})}}{b_2^{(\mathrm{I})}}, \quad t_2^{(2)} = \frac{b_2^{(\mathrm{II})}}{b_2^{(\mathrm{I})}}, \tag{21}$$

where $r_{3,4}^{(2)}$ and $t_{1,2}^{(2)}$ describe, respectively, reflection and transmission of the incident mode $\alpha = 2$ into the modes $\alpha = 3, 4$ and $1, 2$ (note that $r_3^{(2)}, t_1^{(2)}$ correspond to mode conversion of the fast mode $\alpha = 2$ into the slow modes $\alpha = 1, 3$). The reflection and transmission coefficients, referred to the Stroh-normalized representation of partial modes (see equation (6)), are related to the coefficients in equation (21) as

$$R_3^{(2)} = -\mathrm{i}\frac{C_2}{C_1}r_3^{(2)}, \quad R_4^{(2)} = -\mathrm{i}r_4^{(2)}, \quad T_1^{(2)} = \frac{C_2}{C_1}t_1^{(2)}, \quad T_2^{(2)} = t_2^{(2)}. \tag{22}$$

Figure 2. Possible patterns of the dependence $\eta(v^{-1})$ for an orthorhombic material with $c_{11}, c_{22} > c_{66}$ and $c_{12} > 0$. Case (a): $c_{11}c_{22} - c_{12}^2 > c_{66}(c_{12} + c_{22})$, in the presence or absence of the $X$-axial concavity on the outer slowness sheet; case (b): $c_{11}c_{22} - c_{12}^2 < c_{66}(c_{12} + c_{22})$ (the concavity is ensured).

In the forthcoming derivations the normalized form (22) will be adhered to. The conditions of zero of tangential tractions at the interfaces of substrate I and substrate II, taken in conjunction with equations (13) and (22), furnish the connections

$$R_3^{(2)} = \pm \mathrm{i}\sqrt{\eta}(1 + \mathrm{i}R_4^{(2)}), \quad T_1^{(2)} = \mp \sqrt{\eta}\, T_2^{(2)}, \tag{23}$$

in which the upper or lower sign is to be selected, depending on whether the value $L_{2x}/L_{1x} = -L_{1y}/L_{2y}$ is equal, respectively, to $\sqrt{\eta}$ or $-\sqrt{\eta}$. Continuity of the energy-flux normal component yields the identity

$$|R_3^{(2)}|^2 + |R_4^{(2)}|^2 + |T_1^{(2)}|^2 + |T_2^{(2)}|^2 = 1. \tag{24}$$

By equations (18), (21), (22), $R_4^{(2)} = -\mathrm{i}Q_{21}/Q_{11}$ and $T_2^{(2)} = 1/Q_{11}$, where $\mathbf{Q} = \mathbf{W}_{en}\mathbf{W}^{N-1}\mathbf{W}_{ex}$. Implementing the required calculations, the following relations are reached:

$$R_4^{(2)} = \eta \frac{\mathrm{i}\cos(NK_2h) - \Gamma S_N^{(2)}}{(1+\eta)\cos(NK_2h) - \mathrm{i}\Omega S_N^{(2)}}, \quad T_2^{(2)} = \frac{1}{(1+\eta)\cos(NK_2h) - \mathrm{i}\Omega S_N^{(2)}}, \tag{25}$$

where

$$\Gamma = \frac{\cos(k_{1y}h)\cos(k_{2y}h) - \eta\sin(k_{1y}h)\sin(k_{2y}h) - 1}{\sin(k_{1y}h) + \eta\sin(k_{2y}h)}, \tag{26}$$

$$\Omega = \frac{(1+\eta^2)\sin(k_{1y}h)\sin(k_{2y}h) + \eta\{1 - \cos[(k_{1y} + k_{2y})h]\}}{\sin(k_{1y}h) + \eta\sin(k_{2y}h)},$$

Further manipulation yields

$$|R_4^{(2)}|^2 = \eta^2 \frac{1 + \Phi(S_N^{(2)})^2}{(1+\eta)^2 + \eta^2\Psi(S_N^{(2)})^2}, \quad |T_2^{(2)}|^2 = \frac{1}{(1+\eta)^2 + \eta^2\Psi(S_N^{(2)})^2}, \tag{27}$$

where

$$\Phi = \frac{\{1 - \cos[(k_{1y} - k_{2y})h]\}\{1 - \cos[(k_{1y} + k_{2y})h]\}}{[\sin(k_{1y}h) + \eta\sin(k_{2y}h)]^2}, \quad \Psi = \frac{\{1 - \cos[(k_{1y} - k_{2y})h]\}^2}{[\sin(k_{1y}h) + \eta\sin(k_{2y}h)]^2}. \tag{28}$$

Once $R_4^{(2)}$, $T_2^{(2)}$ are determined, the coefficients $R_3^{(2)}$, $T_1^{(2)}$, associated with conversion into the slow reflected and transmitted modes, follow from equation (23).

Provided that the slow mode $\alpha = 1$ is incident in substrate I, the corresponding coefficients $R_3^{(1)}$, $T_1^{(1)}$ and $R_4^{(1)}$, $T_2^{(1)}$ may be obtained from the above-cited equations by interchanging indices $\alpha = 2$ and 1 on their right-hand sides, along with replacing $\eta$ by $\eta^{-1}$.

Applying this to equations (27) and (28) gives

$$|R_3^{(1)}|^2 = \frac{1 + \eta^2 \Phi (S_N^{(1)})^2}{(1+\eta)^2 + \eta^2 \Psi (S_N^{(1)})^2}, \quad |T_1^{(1)}|^2 = \frac{\eta^2}{(1+\eta)^2 + \eta^2 \Psi (S_N^{(1)})^2}, \tag{29}$$

where $S_n^{(1)} \equiv \sin(nK_1h)/\sin(K_1h)$, and appropriate redefinition of equation (15) yields the dispersion relation for $\cos(K_1h)$. For the range $\sqrt{\rho/c_{11}} < v^{-1} < \sqrt{\rho/c_{66}}$, where the modes $\alpha = 2, 4$ are inhomogeneous and hence $\eta = \mathrm{i}\eta''$, $k_{2y} = -\mathrm{i}|k''_{2y}| = -\mathrm{i}|p''_2|k_x$, is found that

$$|R_3^{(1)}|^2 = \frac{[\cos(NK_1h) - \Gamma'' S_N^{(1)}]^2}{(\eta'') + [\cos(NK_1h) - \Gamma'' S_N^{(1)}]^2}, \quad |T_1^{(1)}|^2 = 1 - |R_1^{(1)}|^2, \tag{30}$$

where

$$\Gamma'' = \frac{\sin(k_{1y}h)\sinh(|k''_{2y}|h) + \eta''[\cos(k_{1y}h)\cosh(|k''_{2y}|h) - 1]}{\sin(k_{1y}h) + \eta'' \sinh(|k''_{2y}|h)}. \tag{31}$$

Inserting $N = 0$ or, equally, taking the long-wavelength limit $Nh/\lambda \to 0$ yields the reflection and transmission coefficients at the interface between two identical orthorhombic half-spaces in sliding contact (see reference [3]).

## 4. ANALYSIS OF THE REFLECTION AND TRANSMISSION SPECTRA

According to reference [3], acoustic-wave transmission through a single orthorhombic layer, enclosed between arbitrary substrates with sliding contact along interfaces, turns to zero for some particular angles of incidence regardless of frequency, or otherwise for a frequency-dependent angle of incidence satisfying the equation

$$\sin(k_{1y}h) + \eta \sin(k_{2y}h) = 0. \tag{32}$$

The primary interest here is to determine how the effect of transmission cut-off couples with the Bragg-resonance properties of wave diffraction in the periodic system of layers in sliding contact. Apparently, the most drastic features are to be expected for the angles of incidence close to those which provide the total transmission (anti-reflection) independent of frequency. This comes about, in particular, at nearly normal incidence of the fast (quasi-) longitudinal mode $\alpha = 2$. Targeting the latter setting in the first place, the analysis is commenced from the case of incidence of the mode $\alpha = 2$, while incidence of the mode $\alpha = 1$ is considered subsequently. As an example of layers and substrates material, which is to be employed in graphical illustrations of analytical results, the $TiO_2$ tetragonal crystal will be used (the four-fold axis is assumed to be orthogonal to the sagittal plane $XY$), whose elastic constants and density values are taken from reference [14].

### 4.1. THE FAST MODE INCIDENCE

The spectral dependence of the Bloch wave vector $K_2$, described by equation (15), is characterized by the stop bands, within which $K_2$ is complex: $K_2h = \pi l + \mathrm{i}K''_2h$ ($l = 1, 2, \dots$). Their edges are determined by the condition

$$\cos(K_2h) = (-1)^l. \tag{33}$$

which furnishes the equations

$$\sin(k_{1y}h) = 0, \quad \sin(k_{2y}h) = 0,$$

$$\tan\left(\frac{k_{2y}h}{2}\right) + \eta \tan\left(\frac{k_{1y}h}{2}\right) = 0, \tag{34}$$

$$\cot\left(\frac{k_{2y}h}{2}\right) + \eta \cot\left(\frac{k_{1y}h}{2}\right) = 0.$$

Note that the last two of equations (34) coincide at $\eta \neq 0$, $\eta^{-1} \neq 0$ with the dispersion relations for the Lamb waves in a plate with traction-free faces (see reference [4]). Hereafter, when referred to, the set of roots of each of four equations (34) will be enclosed in braces, and supplied with the corresponding subscript $i = 1, \ldots, 4$ and the superscript $(ed)$ and the subscript $i$ $(i = 1, \ldots, 4)$ corresponding to the number of this equation.

Provided that $\eta \neq 0, \eta^{-1} \neq 0$, the values $|R_4^{(2)}|^2, |T_2^{(2)}|^2$ at the edges of stop bands may be evaluated as follows. At $\sin(k_{1y}h) = 0$,

$$|R_4^{(2)}|^2 = 1 - \frac{1 + 2\eta}{(1 + \eta)^2 + N^2 \tan^2(k_{2y}h/2)} = 1 - (1 + 2\eta)|T_2^{(2)}|^2 \tag{35}$$

for $\{k_{1y}h\}_1^{(ed)} = 2\pi l$ (corresponding to $\{k_{2y}h\}_1^{(ed)} = (p_2/p_1)2\pi l$), and a similar equation with tan replaced by cot describes $|R_4^{(2)}|^2, |T_2^{(2)}|^2$ at the stop-band edges $\{k_{1y}h\}_1^{(ed)} = \pi(2l + 1)$. At $\sin(k_{2y}h) = 0$,

$$|R_4^{(2)}|^2 = 1 - \frac{1 + 2\eta}{(1 + \eta)^2 + \eta^2 N^2 \tan^2(k_{1y}h/2)} = 1 - (1 + 2\eta)|T_2^{(2)}|^2 \tag{36}$$

for $\{k_{2y}h\}_2^{(ed)} = 2\pi l$, while replacing tan by cot in equation (36) yields $|R_4^{(2)}|^2, |T_2^{(2)}|^2$ for $\{k_{2y}h\}_2^{(ed)} = \pi(2l + 1)$. The stop-band edges $\{k_{1y}h\}_3^{(ed)}$ and $\{k_{1y}h\}_4^{(ed)}$, determined, respectively, by the third and fourth of equations (34), bring about

$$|R_4^{(2)}|^2 = 1 - \frac{1 + 2\eta}{(1 + \eta)^2\{1 + \sin^2(k_{1y}h)\sin^2(k_{2y}h)/4[\sin(k_{1y}h) + \eta \sin(k_{2y}h)]^2(1 + \eta)^2 N^2\}}$$

$$= 1 - (1 + 2\eta)|T_2^{(2)}|^2. \tag{37}$$

The values of the mode-conversion coefficients $|R_3^{(2)}|^2, |T_1^{(2)}|^2$, taken at the edges of stop bands, are furnished by the relation

$$|R_3^{(2)}|^2 = |T_1^{(2)}|^2 = \eta|T_2^{(2)}|^2, \tag{38}$$

which follows from equations (35)–(37) and (24). According to equation (15), the imaginary part $K_2''$ of the Bloch wave vector turns to infinity within those stop bands, which contain the spectral points satisfying equation (32). At such points, transmission falls to exactly zero due to cutting-off at the back interface of the first layer. In the forthcoming discussion, the stop bands which include and do not include the solutions of equation (32) will be distinguished, by terming them cutting-off and ordinary stop bands respectively.

Consider the evolution of reflection and transmission spectra with variation of the angle of incidence $\theta_2$ of the mode $\alpha = 2$ from zero. In orthorhombic materials with $c_{11}, c_{22} > c_{66}$ and $c_{12} > 0$, the parameter $\eta$ increases from $\eta = 0$ at $\theta_2 = 0$ $(v^{-1} = 0)$ up to some maximum

value and then decreases back to $\eta = 0$ at $\theta_2 = \pi/2$ ($v^{-1} = \sqrt{c_{11}/\rho}$) (see Figure 2). Exactly normal incidence ($\theta_2 = 0$) entails total transmission into the same wave branch: $|T_2^{(2)}| = 1$, $R_4^{(2)} = 0$, $T_1^{(2)} = 0$, $R_3^{(2)} = 0$, regardless of frequency. At nearly normal incidence $\theta_2 \ll 1$, equation (32) yields transmission zeros at the set of points $\{k_{1y}h\}_c$,

$$\{k_{1y}h\}_c \approx (-1)^{n-1}\eta \sin\left(\sqrt{\frac{c_{66}}{c_{22}}}\,\pi n\right) + \pi n \ (n = 1, 2, \dots), \tag{39}$$

where $k_{2y}/k_{1y}$ is approximated by $\sqrt{c_{66}/c_{22}}$, and

$$\eta \approx \left(\frac{c_{66}}{c_{22}}\right)^{3/2}\left(\frac{c_{22} - c_{66}}{c_{12} + c_{22}}\right)^2 \theta_2^2 \ll 1. \tag{40}$$

The points in equation (39) lie within the narrow nearly periodic cutting-off bands, which are located near zeros of $\sin(k_{1y}h)$ (thus prompting the use of $k_{1y}h$ as a suitable variable for graphical display of the spectra; see Figures below). The edges of successive $n$th cutting-off bands, related to $n = 2l$ and $2l + 1$ in equation (39), are, respectively,

$$\{k_{1y}h\}_1^{(ed)} = 2\pi l,\ \{k_{1y}h\}_4^{(ed)} \approx 2\pi l - 2\pi \tan\left(\sqrt{\frac{c_{66}}{c_{22}}}\,\pi l\right) \tag{41}$$

and

$$\{k_{1y}h\}_1^{(ed)} = (2l + 1)\pi, \quad \{k_{1y}h\}_3^{(ed)} \approx (2l + 1)\pi - 2\eta \cot\left[\sqrt{\frac{c_{66}}{c_{22}}}\,\pi\left(l + \frac{1}{2}\right)\right], \tag{42}$$

where the roots $\{k_{1y}h\}_{4,3}^{(ed)}$ of the fourth and third of equations (34) respectively are approximated under the reservation that $l(k_{2y}/k_{1y}) \approx l\sqrt{c_{66}/c_{22}}$ is not close to an integer number. Values of the Bloch wave-vector $K_2$ at the opposite edges of each cutting-off band differ by $\pi$, which may be interpreted as a result of the U-process ("umklapp") in terms of the reduced Brillouin zone, see e.g., reference [15].

According to equations (35)–(37), the cutting-off bands in equations (41) and (42) on gradually varying spectral width $\Delta(k_{1y}h)$ entail corresponding abrupt drops of the transmission rate $|T_2^{(2)}|^2$ to zero, and maximums of the reflection rate $|R_4^{(2)}|^2$ with the envelope approximated by equation (35). These transmission dips and reflection peaks come about in the corresponding spectra, shown in Figure 3, as successive packs of $T_n$ bands, which repeat themselves with salient similarity. The "quasiperiod" is $T_n = 2C_1$, where $C_1$ results from the ratio of the least integers $C_2/C_1$ which satisfactorily approximates the ratio $k_{2y}/k_{1y}$ (for, the case displayed in Figure 3, $k_{2y}/k_{1y} \approx 0{\cdot}81 \approx C_2/C_1 = 4/5$, so that $T_n = 10$). From equations (41) and (42), the cutting-off bands, which are located closer to the borders of each pack, are narrower and entail transmission drops and reflection peaks with the width of the order $\Delta(k_{1y}h) \sim \eta$. The cutting-off bands lying in the middle of a pack, where $l(k_{2y}/k_{1y})$ is about an integer, are noticeably wider, and hence so do corresponding transmission dips and reflection peaks. By equations (35)–(37), they become steeper and, thereby, increasingly broader with increasing $N$ (Figure 3(b)), which is due to the diffraction effect.

The ordinary stop bands at $\theta_2 \ll 1$ group near zeros of sin $(k_{2y}h)$. The edges of the $m$th band ($m = 1, 2, \dots$) are the point $\{k_{2y}h\}_2^{(ed)} = \pi m$ and the root of the third or fourth

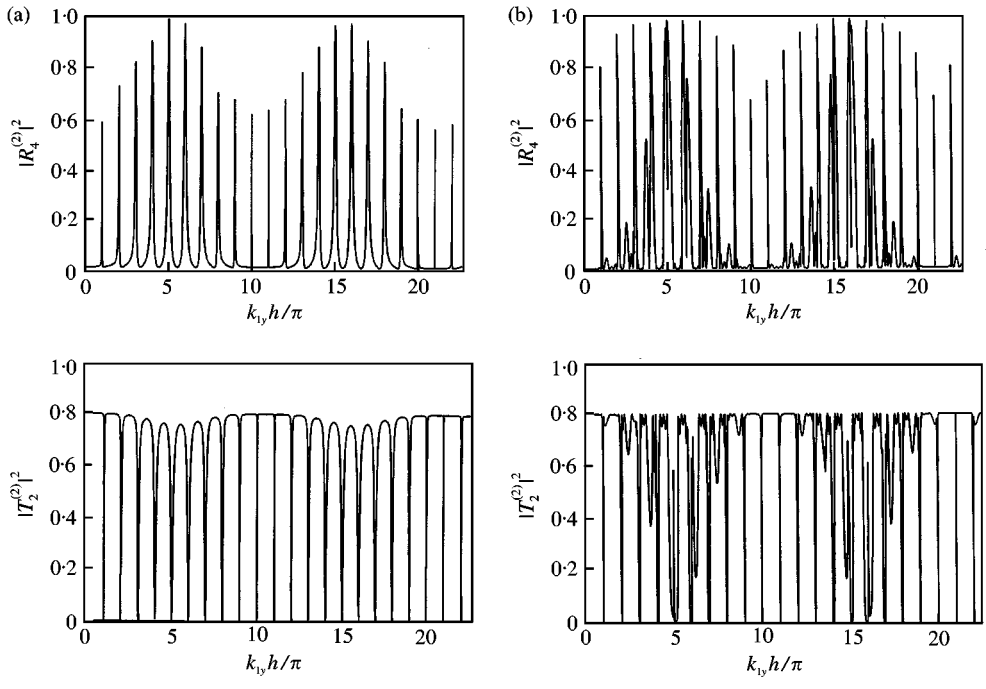


Figure 3. Spectra of reflection and transmission rates $|R_4^{(2)}(k_{1y}h)|^2$, $|T_2^{(2)}(k_{1y}h)|^2$ for the fast mode $\alpha = 2$ incidence at the angle $\theta_2 = 5^\circ$ upon a single layer (a) and five layers (b) of the $TiO_2$ crystal, for which $\eta \approx 0{\cdot}12$, $k_{2y}/k_{1y} \approx 0{\cdot}81$ at $\theta_2 = 5^\circ$.

equation (34) at odd or even $m$ respectively. From equations (36) and (37), at $\eta^2 N^2 \sim \theta_2^2 N^2 \ll 1$ the ordinary stop bands do not manifest themselves in reflection—transmission (Figure 3(a)). Provided that $\eta^2 N^2$ is not a small parameter, the reflection and transmission spectra contain markedly pronounced secondary extremums related to ordinary stop bands (Figure 3(b)). Their envelope, approximated by equation (36), has the quasi-period $T_m = 2C_2$ in terms of band's order $m$, where the integer $C_2$ is defined above ($T_m = 8$ in Figure 3). The extremums, which are located in the middle of quasi-periodic packs close to cutting-off extremums, are substantially amplified. Note that the concept of modulation of the Bragg peaks, underpinned by their position with respect to the cutting-off bands, is different from the case of perfectly bonded layers, when the modulation is governed by the modal coupling [16] or by a ratio of widths of layers in a cell [11, 17].

Thus, the spectra of coefficients $|R_4^{(2)}|^2$, $|T_2^{(2)}|^2$ at nearly normal incidence of the fast mode represent a group o sharp principal extremums, which are associated with the cutting-off bands, and, when $\eta^2 N^2$ is not too small, a group of secondary extremums, related to the ordinary stop bands and generally increasing with growing $\eta^2 N^2$. The peaks of reflection reach almost unit height against nearly zero background, and transmission drops abruptly to zero against background close to unity. This signifies sharp filtering features of reflection–transmission under the given conditions. As regards coefficients $R_3^{(2)}$, $T_1^{(2)}$, which describe conversion of the incident fast mode into slow ones, they are essentially attenuated due to the presence of the small factor $\sqrt{\eta} \sim \theta_2$ in equation (23) (see also equation (38)).

Consider further deviation from normal incidence. Ensuing increase of $\eta$ moves the cutting-off points $\{k_{1y}h\}_c$ and the band edges $\{k_{1y}h\}_{3,4}^{(ed)}$ away from zeros of $\sin(k_{1y}h)$, so that the cutting-off bands are broadened. At $\eta \leqslant 1$, when equations (39), (41) and (42) are no longer valid, these bands become essentially aperiodic and their widths become different.

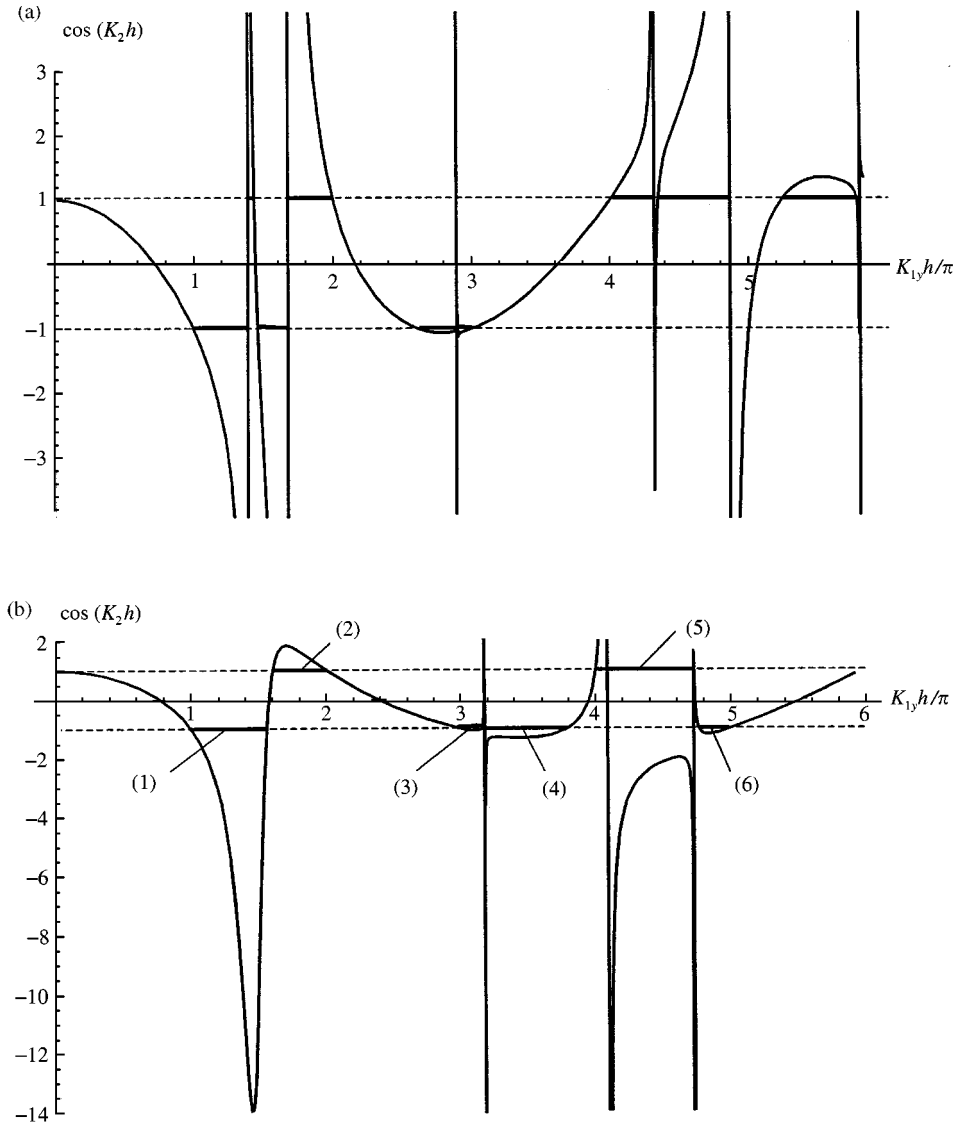


Figure 4. Dependence of $\cos(K_2h)$ on $k_{1y}h$ at $\eta \approx 0{\cdot}95$ (a) and at $\eta \approx 1{\cdot}1$ (b), showing the transformation of the Bloch spectrum at passing the threshold value $\eta = 1$, attained in the case of the $TiO_2$ crystal. The stop bands are marked and, in Figure 4(b), indexed.

Some neighboring stop bands tend to each other, thus narrowing the propagation zones between them. At $\eta = 1$, the last two of equations (34) coalesce, and their roots appear among solutions of equation (32). As a result, the value $\eta = 1$, provided it is attained for a given material, is a threshold for a drastic reshuffle of the structure of the Bloch spectrum (Figure 4). In particular, a pair of cutting-off bands, closely situated at $\eta \leqslant 1$, may merge at $\eta > 1$ into a single one, containing two cutting-off points (such a double cutting-off band is labeled as band 5 in Figure 4(b)). Continuing the increase of $\eta > 1$, along with $\sin(k_{2y}h)$ increasing more slowly in comparison with $\sin(k_{1y}h)$ due to decreasing $k_{2y}/k_{1y}$, entails some pairs of cutting-off points vanishing and thereby results in transformation of corresponding double cutting-off bands into pairs of ordinary stop bands, separated initially by a very

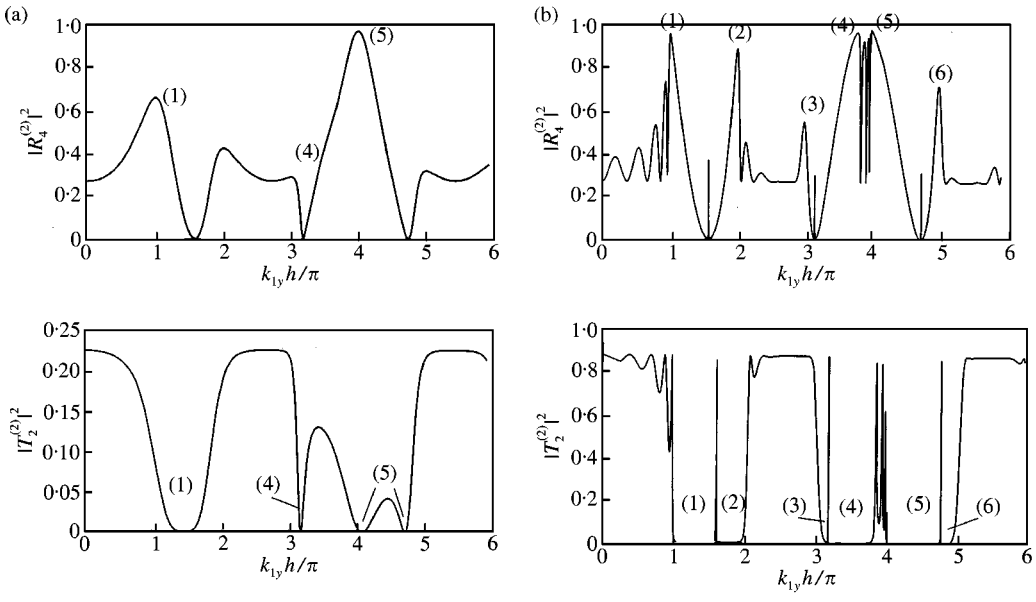


Figure 5. Spectra of reflection and transmission rates $|R_4^{(2)}(k_{1y}h)|^2$, $|T_2^{(2)}(k_{1y}h)|^2$ for the fast mode $\alpha = 2$ incidence at the angle $\theta_2 = 60^\circ$ upon a single layer (a) and five layers (b) of the $TiO_2$ crystal ($\eta \approx 1{\cdot}1$, $k_{2y}/k_{1y} \approx 0{\cdot}10$). Numbers in parentheses correspond to the indices of the stop bands in Figure 4(b).

narrow propagation band. Hence, reducing the number of cutting-off bands and more frequent appearance of the ordinary stop bands are the general features of the Bloch spectrum at increasing $\eta > 1$. However, insofar as the discrepancy between $\sin(k_{1y}h)$ and $\eta \sin(k_{2y}h)$ within the ordinary stop band emerging from the cutting-off one is small, the imaginary part $K_2''$ of the Bloch wave vector may reach a considerably large value, which results in almost zero transmission which is virtually indistinguishable from that at cutting-off points. For example, see the ordinary (finite) stop band 1 in Figure 4(b) and the corresponding transmission dip in Figure 5.

Comparing the Bloch spectrum (Figure 4(b)) and the spectra $|R_4^{(2)}|^2$, $|T_2^{(2)}|^2$, taken for the same value $\eta \geqslant 1$ at $N = 1$ and 5 (Figures 5(a) and (b), respectively), shows the impact of diffraction resonance at growing number $N$ of layers. At $N = 1$ (Figure 5(a)), the structure of reflection and transmission spectra is stipulated mostly by the cutting-off points. At $N^2 \gg 1$, in accordance with equations (35)–(37), both the cutting-off and the ordinary stop bands reveal themselves significantly. Figure 5(b) shows almost perfect transmission cut-off inside wide step-wise dips with in places embedded sharp peaks related to narrow propagation zones. Such a drop of plane-wave transmission within a spectral range of the spectral width $\Delta(k_{1y}h)$ of the order of unity provides almost exactly zero transmission for an acoustic beam radiated by a source of the size $w \geqslant h$, which is not too stringent a restriction. In turn, the maxima of reflection rate $|R_4^{(2)}|^2$ within the cutting-off and the ordinary stop bands come about at $N^2 \gg 1$ as steep and distinct peaks. Drops of $|R_4^{(2)}|^2$ to nearly zero value occur within narrow propagation zones due to $\cos[(k_{1y} + k_{2y})h]$ tending to zero, so that in equation (27) $\Phi \ll 1$, while $\Psi \gg 1$ because of its small denominator near the cutting-off points. Note that, according to equation (38), at $\eta \sim 1$ the values of coefficients $|R_3^{(2)}|$, $|T_1^{(2)}|$, associated with mode conversion, are close to that of $|T_2^{(2)}|$ (see also equation (24)).

On reaching the maximum value, $\eta$ begins decreasing with further increasing $\theta_2$ (Figure 2). This generally entails reverse character of the reflection and transmission spectra.

At $\theta_2 \to \pi/2$ and $\eta^2 N^2 \ll 1$, the spectral dependencies of the coefficients $|R_4^{(2)}|$ and $|T_2^{(2)}|$ consist of, respectively, narrow peaks and dips within the cutting-off bands, again grouping near zeros of $\sin(k_{1y}h)$. The grazing longitudinal mode ($\theta_2 = \pi/2$, hence $\eta = 0$) "does not feel" sliding-contact interfaces between identical media, which corresponds to the limit of total transmission $|T_2^{(2)}| = 1$, $R_4^{(2)} = 0$, $T_1^{(2)} = 0$, $R_3^{(2)} = 0$ independent of frequency, similar to the case of normal incidence.

### 4.2. THE SLOW MODE INCIDENCE

Suppose now that the slow mode $\alpha = 1$ is incident at the angle $\theta_1$ (see equations (29)–(31)). The angles of incidence, which yield zeros of $\eta$ (Figure 2), provide $|R_3^{(1)}| = 1$, $R_4^{(1)} = 0$, $T_1^{(1)} = 0$, $T_2^{(1)} = 0$ for any frequency, due to transmission cut-off on the substrate I interface. On the other hand, the angle of incidence

$$\theta_1^{(0)} = \operatorname{arccot} \sqrt{\frac{c_{11} + c_{12}}{c_{22} + c_{12}}}, \tag{43}$$

which is associated with the pole $v_0^{-1}$ of $\eta(v^{-1})$, entails total transmission $R_3^{(1)} = 0$, $R_4^{(1)} = 0$, $|T_1^{(1)}| = 1$, $T_2^{(1)} = 0$ independent of frequency ($\theta_1^{(0)} = 45^\circ$, if the sagittal plane is orthogonal to the four- or six-fold symmetry axis). At angles of incidence $\theta_1$ close to $\theta_1^{(0)}$, when $\eta^{-1} \sim |\theta_1 - \theta_1^{(0)}|^2 \ll 1$, it is suitable to present equation (32) in the form

$$\sin(k_{2y}h) + \eta^{-1} \sin(k_{1y}h) = 0, \tag{44}$$

which matches insertion of the external factor $\eta^2$ into $\Phi^2$ and $\Psi^2$ in equation (29). Further along these lines, one may interchange indices $\alpha = 1$ with 2 and replace $\eta$ by $\eta^{-1}$ in equations (35)–(37), (39), (41) and (42). If the slowness sheet of the slow sagittal wave branch in a given material possesses the $X$-axial concavity and the pole $v_0^{-1}$ lies in the range $\sqrt{\rho/c_{66}} < v^{-1} < v_L$ (see Figure 2(b)), it then follows that the spectral dependencies $|R_3^{(1)}|$, $|T_1^{(1)}|$ on $k_{2y}h$ manifest basically the same features at $|\theta_1 - \theta_1^{(0)}| \ll 1$ as the corresponding dependencies of $|R_4^{(2)}|$, $|T_2^{(2)}|$ on $k_{1y}h$ at nearly normal incidence $\theta_2 \ll 1$ of the mode $\alpha = 2$. The principal dissimilarity of corresponding spectra in Figure 3(b) and 6 is related to the quasi-periods of stop bands which indeed change due to a different value of $k_{2y}/k_{1y}$.

Alternatively, the pole $v_0^{-1}$ for a given material may come about in the range $\sqrt{\rho/c_{11}} < v^{-1} < \sqrt{\rho/c_{66}}$, in which the modes $\alpha = 2$, 4 are inhomogeneous and hence values $k_{2y}$ and $\eta$ are purely imaginary (see Figure 2(a)). Then equation (44) may be specified as

$$\sinh(|k''_{2y}|h) + (\eta'')^{-1} \sin(k_{1y}h) = 0. \tag{45}$$

In such a case, for the angles of incidence $\theta_1$ close to $\theta_1^{(0)}$, either there is only a finite number of cutting-off points and hence cutting-off bands, which lie in the long-wavelength part of the spectrum, or there may be no cutting-off points and bands at all. The cutting-off bands may arise in the long-wavelength spectral domain and increase in number with further variation of $\theta_1$ away from $\theta_1^{(0)}$ (hence, increasing $(\eta'')^{-1}$), but their number remains finite as long as $v^{-1}$ is kept within the range $\sqrt{\rho/c_{11}} < v^{-1} < \sqrt{\rho/c_{66}}$.

In the presence of the $X$-axial concavity on the outer slowness sheet, the reflection and transmission gain also specific features at the incidence of the mode $\alpha = 1$ at

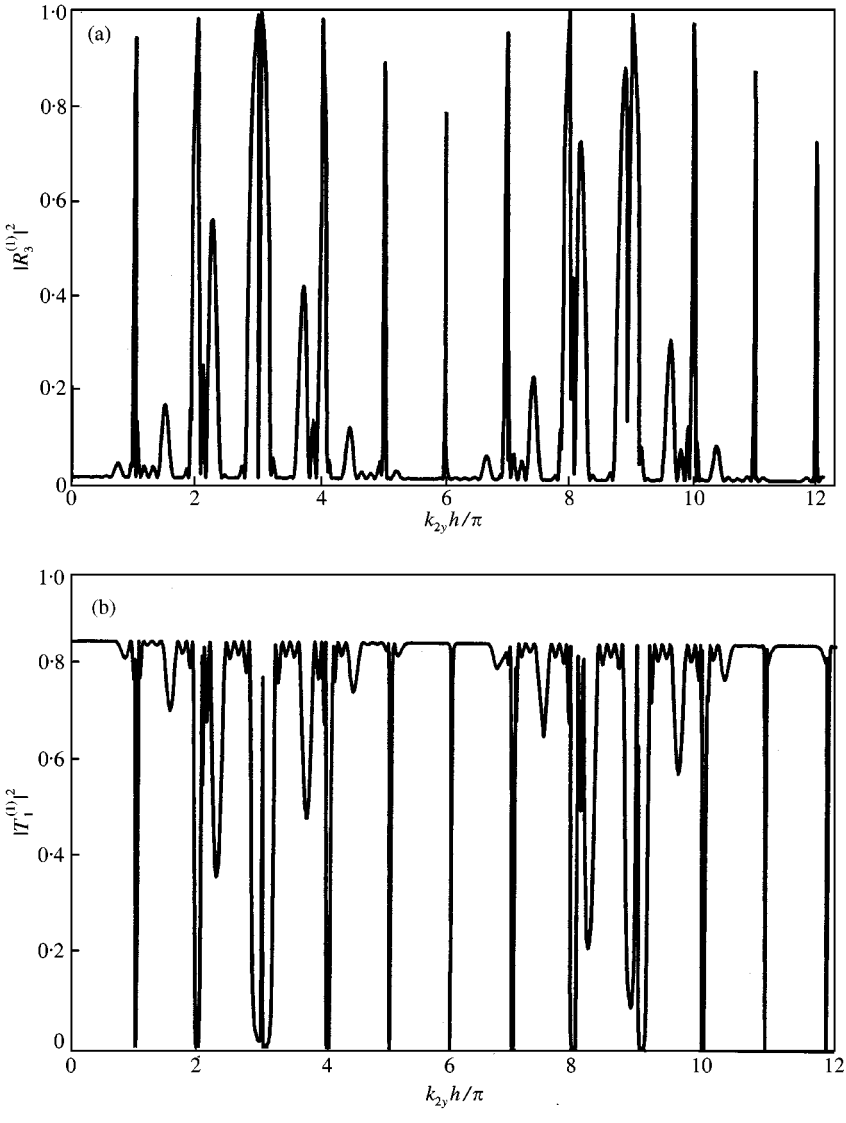


Figure 6. Spectra of reflection and transmission rates $|R_3^{(1)}(k_{2y}h)|^2$, $|T_1^{(1)}(k_{2y}h)|^2$ for the slow mode $\alpha = 1$ incidence upon five layers of the $TiO_2$ crystal at the angle $\theta_1 = \theta_1^{(0)} + 3^\circ$. In the given case, $\theta_1^{(0)} = 45^\circ$ corresponds to the value $v_0^{-1}$ lying in the range $\sqrt{\rho/c_{66}} < v_0^{-1} < v_L$, and $\eta^{-1} \approx 0{\cdot}089$, $k_{1y}/k_{2y} \approx 0{\cdot}74$.

the angle

$$\theta_1^{(c)} = \operatorname{arccot} \sqrt{\frac{(c_{12} + c_{66})^2 - c_{22}(c_{11} - c_{66})}{c_{22}c_{66}}}, \tag{46}$$

which corresponds to $v^{-1} = \sqrt{\rho/c_{66}}$. In the case of the sliding-contact interface between two identical orthorhombic half-spaces, the angle of incidence $\theta_1^{(c)}$ provides total transmission $R_3^{(1)} = 0$, $T_1^{(1)} = 1$, accompanied by the excitation of transverse modes travelling along the interface ($R_4^{(1)} = 0$, $T_2^{(1)} = 0$, but $r_4^{(1)}, t_2^{(1)} \neq 0$ in view of divergence of the

Stroh normalization (6) for grazing modes). On the other hand, fulfilment of equation (44) at $v^{-1} = \sqrt{\rho/c_{66}}$ due to $\eta^{-1} \sim p_2 = 0$ and $k_{2y} = p_2 k_x = 0$ ensures cutting-off of transmission through an orthorhombic layer enclosed between arbitrary substrates with elastic properties different from those of the layer [3]. In the present case of an identical material of layers and substrates, neither of these two phenomena persists in a pure state. From equation (29), exactly at $\theta_1 = \theta_1^{(c)}$

$$|R_3^{(1)}|^2 = \frac{F}{1+F} = F|T_1^{(1)}|^2, \tag{47}$$

where

$$F = \frac{[1-\cos(k_{1y}h)]^2}{[\sin(k_{1y}h) + (\eta p_2)k_x h]^2} \frac{\sin^2(Nk_{1y}h)}{\sin^2(k_{1y}h)}. \tag{48}$$

Since the denominator of the first ratio on the right-hand side of equation (48) largely exceeds the numerator, there is practically total transmission at $\theta_1 = \theta_1^{(c)}$ for any frequency, except for the resonance spectral zones, which are attached to the set of points $\{k_{1y}h\} = \pi(2l+1)$ $(l = 0, 1, \dots)$ and are associated with the second ratio in equation (48). Within these zones of the spectral width $\Delta(k_{1y}h) \approx 2\pi/N$, the reflection rate has peaks with the heights

$$|R_3^{(1)}|^2 = \left[\frac{2Np_1}{(\eta p_2)\pi(2l+1)}\right]^2, \tag{49}$$

decreasing on increasing the peak number $2l+1$, while the transmission rate $|T_1^{(1)}|^2$ has corresponding drops (Figure 7). Note that there are no resonances at $\{k_{1y}h\} = 2\pi l$ due to the vanishing numerator of the first ratio in equation (48). At the same time, a slight deviation of the incidence angle $\theta_1$ from $\theta_1^{(c)}$ provides a non-zero value $k_{2y}$, and then equations (47) and (48) remain approximately valid only in the long-wavelength spectral domain, in which $k_{2y}h = p_2 k_x h \ll 1$. Outside this range, the reflection peaks emerge at the points $\{k_{1y}h\} = 2\pi l$ and the modulation of the reflection spectrum by the sinusoidal envelope reveals itself clearly (see the inset of Figure 7).

## 5. SUMMARY

The propagation of sagittal acoustic waves through the system of identical orthorhombic layers in sliding contact, enclosed between substrates of the same material, is considered. The substantial difference in reflection and transmission spectra when compared with the case of perfectly bonded multilayers is due to the Bragg phenomenon combining with the effect of transmission cut-off, which pertains particularly to the case of sliding contact. This coupling entails new features of the concept of stop bands, which relates the reflection increase to a rising imaginary part of the Bloch vector. The imaginary part, remaining finite within the ordinary stop bands, now reaches infinity within the stop bands, termed cutting-off bands. Especially, abrupt transformation of reflection and transmission occurs at small deviation of $\Delta\theta$ from the normal incidence of the fast mode $\alpha = 2$ or else from the angle of incidence (equation (43)) of the slow mode $\alpha = 1$ (the latter option presumes the presence of concavity on the slowness sheet of slow sagittal wave branch). Then $\Delta\theta = 0$

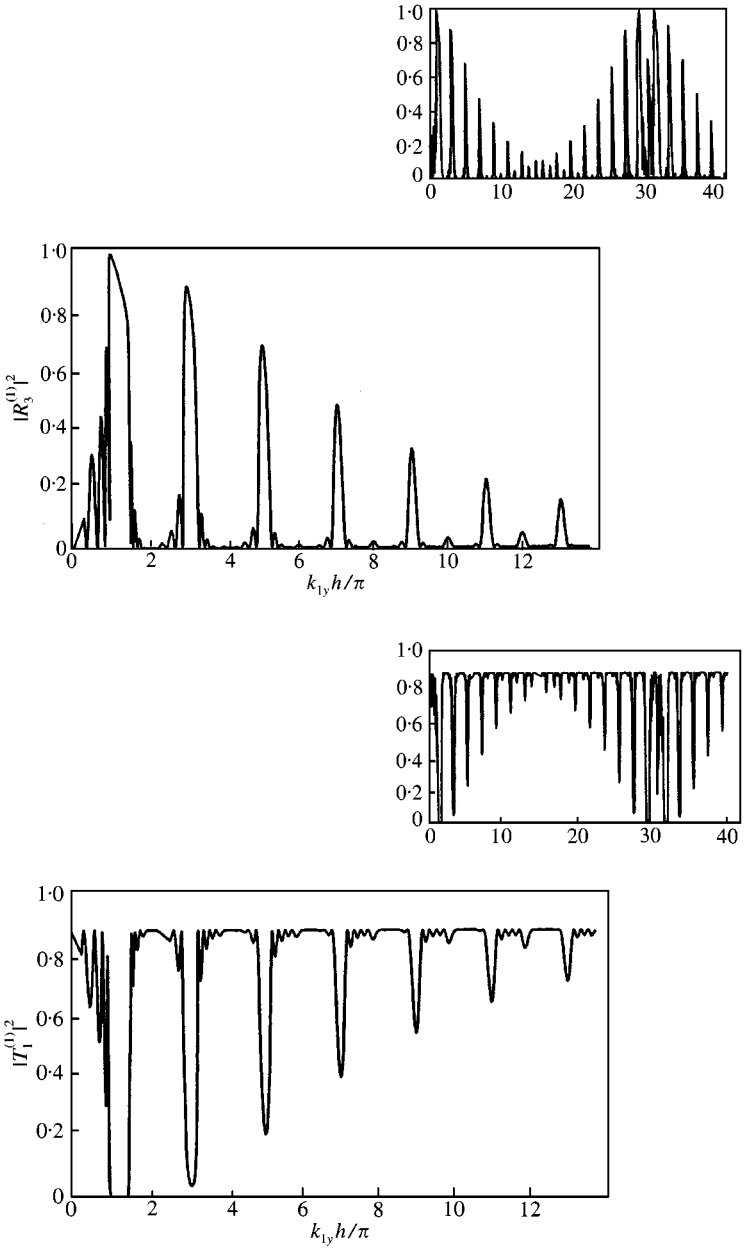


Figure 7. Spectra of reflection and transmission rates $|R_3^{(1)}(k_{1y}h)|^2$, $|T_1^{(1)}(k_{1y}h)|^2$ for the slow mode $\alpha = 1$ incidence upon five layers of the $TiO_2$ crystal at the angle $\theta_1 = \theta_1^{(c)} + \pi 10^{-3}$, where $\theta_1^{(c)} = 34^\circ$ corresponds to $v^{-1} = \sqrt{\rho/c_{66}}$ due to the $X$-axial concavity on the outer slowness sheet for $TiO_2$. Here $\eta \approx 14$, $k_{2y}/k_{1y} \approx 0{\cdot}03$.

corresponds to total transmission independent of frequency, while at $|\Delta\theta| \ll 1$ the transmission spectrum acquires nearly periodic sharp principal dips to zero, accompanied at $|\Delta\theta|^2 N^2 \sim 1$ by secondary minimum, and the reflection spectrum gains corresponding principal and secondary peaks with modulated heights. The spectra evolve with variation of the angle of incidence $\theta$, and then they undergo a drastic change near the point $\eta = 1$, which implies mutual transformation of the ordinary stop bands and cutting-off bands. This

cross-over leads to step-wise dips of transmission to almost zero, which persists at $N^2 \gg 1$ within significantly wide stop bands, and to a rapid change of reflection from about unit value to nearly zero and back within narrow propagation zones.

## ACKNOWLEDGMENT

This work has been supported by the Russian Foundation for Basic Research under the grant 97-02-16338. The authors are grateful to Professor V.I. Alshits for useful discussions.

## REFERENCES

1. P. A. MARTIN 1990 in *Ultrasonic Nondestructive Evaluation* (S. K. Datta, J. D. Achenbach and Y. S. Rajapakse, editors). Amsterdam: North-Holland. Thin interfacial layers: adhesives, approximations and analysis.
2. D. M. BARNETT, S. D. GAVAZZA and J. LOTHE 1988 *Proceedings of the Royal Society of London A* **415**, 389–419. Slip waves along the interface between two anisotropic elastic half-spaces in sliding contact.
3. A. L. SHUVALOV and A. S. GORKUNOVA 1999 *Wave Motion* **30**, 345–365. Cutting-off effect at reflection-transmission of plane acoustic waves in anisotropic media with sliding-contact interfaces.
4. A. H. NAYFEH 1995 *Wave Propagation in Layered Anisotropic Media*. Amsterdam–New York: North-Holland.
5. T. C. T. TING 1996 *Anisotropic Elasticity*. New York: Oxford University Press.
6. M. J. K. MUSGRAVE 1970 *Crystal Acoustics*. San Francisco: Holden-Day.
7. A. L. SHUVALOV and A. G. EVERY 1996 *Physics Reviews B* **53**, 14 906–14 916. Curvature of acoustic slowness surface of anisotropic solids near symmetry axes.
8. B. DJAFARI-ROUHANI, L. DOBRZYNSKI, O. HARDOUIN DUPARC, R. E. CAMLEY and A. A. MARADUDIN 1983 *Physics Reviews B* **28**, 1711–1719. Sagittal elastic waves in infinite and semi-infinite superlattices.
9. D. A. SOTIROPOULOS and A. F. VAKAKIS 1995 *Journal of Sound and Vibration* **187**, 178–183. On the propagation zones of weakly bonded layered materials.
10. M. SCHOENBERG 1984 *Wave Motion* **8**, 303–320. Wave propagation in alternating solid and fluid layers.
11. V. I. ALSHITS and A. L. SHUVALOV 1995 *Journal of Applied Physics* **77**, 2659–2665. Resonant reflection and transmission of shear elastic waves in multilayered piezoelectric structures.
12. A. M. B. BRAGA and G. HERRMANN 1992 *Journal of the Acoustical Society of America* **91**, 1211–1227. Floque waves in anisotropic periodically layered composites.
13. A. YARIV and P. YEH 1984 *Optical Waves in Crystals*. New York: Wiley.
14. F.-J. BIRCH 1960 *Geophysics Research* **65**, 3885.
15. CH. KITTEL 1975 *Introduction to Solid State Physics*. New York, London, Sydney, Toronto: John Wiley and Sons; fourth edition.
16. S. TAMURA and J. P. WOLFE 1987 *Physics Reviews B* **35**, 2528–2531. Coupled-mode stop bands of acoustic phonons in semiconductor superlattices.
17. A. L. SHUVALOV and A. S. GORKUNOVA 1999 *Physics Reviews B* **59**, 9070–9077. Transverse acoustic waves in piezoelectric and ferroelectric antiphase superlattices.